Caliphate Journal of Science & Technology (CaJoST)

ISSN: 2705-313X (**PRINT**); 2705-3121 (**ONLINE**) **Research Article**

Open Access Journal available at: https://cajostssu.com and https://www.ajol.info/index.php/cajost/index

DOI: https://dx.doi.org/10.4314/cajost.v4i2.7

Article Info

Received: 17th March 2022

Revised: 10th May 2022

Accepted: 20th May 2022

Soil Remediation Using Zero-Valent Iron Nano-Particle Modified with *Spondias Mombin* Leaves Extract

Blessing O. Ayomide, Gloria U. Obuzor, and Chidi Obi*

Department of Pure and Industrial Chemistry, Faculty of Science, University of Port Harcourt, Rivers State, Nigeria.

***Corresponding author's email:**

chidi.obi@uniport.edu.ng

Zero-valent iron nano-particle (nZVI) was modified with *Spondias mombin* (*Sm*) leaves extract (*Sm*-nZVI) for the removal of total petroleum hydrocarbons (TPH), total hydrocarbon content (THC), and polycyclic aromatic hydrocarbons (PAHs) from contaminated soil. Advanced analytical tools such as Fourier Transform Infra-Red (FT-IR) Spectrophotometer, Scanning Electron Microscope(SEM) and X-ray diffractometer (XRD) were used to characterize the biosynthesized zero-valent iron nano-sorbent. The Fourier Transform Infra-Red analysis confirmed that the bioactive molecules such as alkaloids, polyphenols, flavonoids, etc. in *Spondias mombin* leaves extract were responsible for the zero-valent iron nanoparticle synthesis and stabilization. The peaks at 2θ equal to 44.9° confirmed zero-valent iron (Fe^0) in *Sm*-nZVI. The micrograph showed an average particle size ranging from 13 nm to 158 nm in *Sm*-nZVI revealing the micro-porosity of the sorbent. The application of *Sm*-nZVI for the removal of organic pollutants with varied effects of experimental parameters such as dosage, contact time and pH were successful. The result showed that the pH value for optimum removal efficiency (%) of THC (77.99%), TPH (75.61%) and PAHs (96.98) was 3.0. The adsorbent dosage for optimum removal efficiency (%) was 0.8 g for THC (79.15%), TPH (80.36%) and PAHs (97.31%) and contact time was 45 min for PAHs (97.86%) and 120 min for THC (83.98%) and TPH (85.54%). The biosynthesized zero-valent iron nano-particle showed higher removal efficiency (%) for PAHs (97.29%). This study reveals *Spondias mombin* zero-valent iron nano-sorbent (*Sm*-nZVI) as an effective and efficient sorbent for remediation of soil ladened with organic pollutants and the likes.

Cite this: *CaJoST*, 2022, 2, 172-182

Keywords: Nano-particle; Phytoremediation; *Spondias mombin*; Analytical tools; Soil.

1. Introduction

In recent years, rising soil contamination problems caused by agricultural and industrial activities have ignited global concern (Ha et al., 2014). Humans are the primary sources of soil contamination, bringing about an accumulation of contaminants in soils that can hit alarming levels (Cachada et al., 2018). All solutes introduced into the soil (environment) as a result of human actions are considered soil contaminants (ISO, 2013). It does not matter whether the concentrations exceed harmful levels or not. When contaminant concentrations reach an unacceptably high level, pollution occurs (Lacatusu, 2000).

Pesticides, petroleum and related products, polycyclic aromatic hydrocarbons (PAHs), heavy metals and chlorophenols all penetrate the water or soil, posing a serious hazard to the fragile natural environment and human health (Hu et al., 2013; Zeng et al., 2013; Tang et al., 2014; Paz-Ferreiro et al., 2018). According to the Status of the World's Soil Resources Report, some contaminants can cause soil acidification and nutrient imbalances which are the two key issues in several areas of the world (FAO and ITPS, 2015). Point sources of contamination include emissions, solid discharge and effluents from vehicle exhaustion, factories, and metals from mining and smelting, as well as non-point sources including pesticide use, soluble salts (synthetic and natural), municipal and industrial waste disposal in agriculture, and improper use of chemical fertilizers (Bhatia et al., 2015).

In Nigeria, however soil pollution emanates from household wastes, agricultural wastes, oil spills, gas flaring, used lubricating oil, etc. Used engine oil usually obtained after servicing and subsequently draining spent oil from automobiles and generator engines is disposed into open soil, water drains and farmland by auto and

generator mechanics with workshops on the roadsides (Adejoro and Oguntimehin, 2017). In addition, the oil refineries and offshore drilling operations also discharge a large amount of sludge, which needs to be properly discarded, or else they result in large-scale contamination of land and water resources. Crude oil, also known as petroleum sludge, is a mixture of complex aromatic, aliphatic, resin hydrocarbons and asphaltene, several of which are known to be poisonous, with some of them being mutagenic and carcinogenic. The soil contamination with toxic total petroleum hydrocarbons (TPH), total hydrocarbon content (THC), and polycyclic aromatic hydrocarbons (PAHs) results into extensive damage to biodiversity of flora and fauna, leading to reduced productivity on land and contamination of ground water (Thapa et al., 2012).

In the light of the above issues, it is imperative to develop a cost-effective and environmentally safe technology for effective remediation of polluted soils (Hu et al., 2013; Shankar et al., 2016; Nnanake-Abasi et al. 2021). Many physical and chemical approaches for contaminated soil remediation have been found to be less cost-effective, and they lead to the production of secondary byproducts that are not environmentally sustainable and necessitate additional effort to manage. The conventional methods of treating contaminated soil include thermal desorption (Vamerali et al., 2010), soil washing/flushing (Dermont et al., 2008; Lemaire et al., 2013), photo-catalysis (Wang et al., 2016; Wu et al., 2017), vitrification (Curiel et al., 2009), and bioremediation (Barnes et al., 2010), however, these methods have a risk of relatively expensive, time-consuming and secondary pollution. Most remediation techniques only transform soil pollutants into their less toxic forms rather than complete removal of toxic substances (Koul and Taak, 2018; Lu et al., 2021).

By comparison, phytoremediation is a plant-based alternative technique for remediation of soil, which could remove degrade, extract, sequester, and stabilize a wide range of soil pollutants. The efficiency of phytoremediation depends strongly on the uptake ability of plants and the bioavailability of pollutants. Nevertheless, the biological availability of pollutants and the endurance capacity of certain plants are limited. However, to solve these drawbacks, the combined remediation strategy using phytoremediation and nanotechnology is an emerging technology (Gil-Diaz et al., 2016; Gong et al*.,* 2017b; Yuting et al., 2020; Mahmoud et al., 2021; Alani et al., 2021; Ari et al., 2022). The plant extract used in this combination strategy is obtained from *Spondias mombin* leaves. *Spondias mombin* belongs to the cashew family called Anacardiaceae. It is a tropical angiospermous tree, which grows up to 22 m high; the leaves are about 20-30 cm long and under hairy. This produces an abundant harvest of pierisrapae fragrant panicle flowers that begin green then becomes a lightweight golden yellow when ripe. It is readily common in Brazil, Nigeria and many other tropical forests of the planet (Leon and Shaw, 1990). In Nigeria, *Spondias mombin* is understood by several names such as Ijikara in Igbo, Iyeye in Yoruba, chabbuli in Fulani, nsukakara in Efik, Tsardarmasar in Hausa etc. (Gill, 1992). Most times, this plant leaves are not properly utilized and eventually shade of and constitute nuisance to the fragile ecosystem.

This study therefore focuses on the investigation of the ability and efficiency of zero-valent iron nano-particle (nZVI) biosynthesized using *Spondias mombin* leaves extract as a stabilizing agent to remediate total petroleum hydrocarbons (TPHs), total hydrocarbon content (THC), and polycyclic hydrocarbons (PAHs) from polluted soil.

2. Methodology

2.1 Collection and Preparation of Plant Sample (*Spondias mombin*)

Fresh leaves of *Spondias mombin* were collected from their natural habitat in Owerri, Imo State of Nigeria in June 2019. The University of Port Harcourt's Department of Plant Sciences and Biotechnology classified and authenticated the leaves. The leaves were washed four times with tap water and rinsed twice with distilled water in order to remove soil, bird droppings, and other impurities. The washed leaves were sun-dried for two weeks in the open air to a constant weight. The dried leaves were pulverized into a fine powder using a National star mechanical blender (model no: NS-y44). The pulverized leaves were duly stored in an air-tight bottle prior extraction. This was labelled *Sm.*

2.2 Aqueous Extraction of *Spondias mombin* Leaves

Distilled water (200 mL) was applied to finely pulverized 50 g *Sm* in a 500 mL conical flask and put in a water bath. The mixture boiled at 90^{o}C for 30 min with constant agitation at interval. After removing the beaker from the water bath, the solution was allowed to cool overnight. Whatman No. 1 filter paper was used to filter the aqueous plant sample. For characterization and further use, the filtrate was held at 4^{o}C in a refrigerator.

2.3 Ethanolic Extraction of *Spondias mombin* Leaves

Finely pulverized dried *Spondias mombin* (25 g) was wrapped with Whatman filter paper (18.5 mm) and placed in the thimble of a Soxhlet extractor fitted to 250 ml round bottom flask containing 200 mL ethanol. After extraction for 72 hrs, the mixture was allowed to cool, and the extract recovered by placing in water bath at 55^{o}C for excess solvent evaporation. The extract (75 mL) was stored in an air-tight sample bottle for further usage.

2.4 Phytochemical Screening of *Spondias mombin* Extract

Preliminary phytochemical screening was performed on the *Sm* extract to identify the presence of various phytochemicals such as alkaloids, steroids, tannins, flavonoids, and saponins, using standard methods such as those defined by Harbone and Baxter (1993), AOAC (1990) and Sofowora (1993).

2.5 Collection and Preparation of Soil Sample

Soil sample was collected with the aid of pre-cleaned auger from an auto-mechanic workshop at Ozuoba, along Choba Road, Port Harcourt, Rivers State at a depth of 55 cm. The soil sample collected placed in a sampling bag, labelled “Crude soil” and immediately transported to the laboratory for analysis. In the laboratory, the soil sample was air dried and screened by passing it through a 2 mm metal mesh, obtaining an amount of 1000 g crude soil sample and stored in glass sample bottle for further analysis.

2.5.1 Determination of PAHs and TPH of Crude Soil and Plant Sample Using GC-FID

The soil sample and pulverized plant samples were collected in clean glass bottles, packed and then stored at the temperatures below 4^{o}C, for a maximum of 7 days prior to extraction using soxhlet extractor and 40 days after extraction prior to analysis (ASTM-D7678). In order to remove moisture, 5 g of anhydrous sodium sulphate was added to each 250 mL extraction bottle before adding the extraction solvent. Each 250 mL extraction bottle received 40 mL of extraction solvent (dichloromethane) and was properly covered with aluminum foil paper. To monitor pressure build-up, the reaction mixtures were swirled or agitated for 2 min while removing the cover and the extract was allowed to settle in 15 min. The extracted mixtures were filtered through 2 g of sodium sulphate and activated silica gel on filter paper. For further calculations, the volume of each extract obtained was reported. An aliquot of the extract was transferred to a vial and guided injected into the gas chromatography. The components were separated via gas chromatography and detected with flame ionization detection (GC-FID).

2.5.2 Determination of THC of the Crude Soil and Plant Sample Using IR Spectrophotometer

The soil sample and pulverized plant samples were collected in clean glass bottles, packed and then stored at the temperature below 4^{o}C, for a maximum of 7 days prior to extraction and 40 days after extraction prior to analysis (ASTM-D7678). Soil portion (5 g) and plant portion (5 g) were weighed into 250 mL extraction bottle each. Every 250 mL extraction bottle received 40 mL of extraction solvent (dichloromethane), which was shaken in a shaking water bath for 5 hrs and allowed to settle for at least 60 min. To remove moisture and non-petroleum hydrocarbons, the extracted mixtures were filtered through a bed of sodium sulphate and activated silica gel using a funnel. The residue was washed and made up with the extracting solvent and filtered through the funnel again. After that, it was moved to a vial to be analysed. The extract's IR absorbance was calculated using a mid-IR Spectrophotometer set to 2930 nm.

2.6 Synthesis of Zero-Valent Iron Nano-particle (nZVI)

The synthesis of nZVI took place in a fume cupboard. A 250 mL of 0.05 M $FeSO_4.7H_2O$ was placed inside three-necked round bottom flask and placed on a magnetic stirrer inside the fume cupboard. Also, 250 mL of 0.1 M $NaBH_4$ was added one drop per 2 s into the $FeSO_4.7H_2O$ solution with the aid of a burette with vigorous stirring at room temperature. Excess $NaBH_4$ was needed for better formation of nZVI. After the few drops of $NaBH_4$ solution, black precipitates immediately appeared with evolution of hydrogen gas and then after 2 min, the intensity of black precipitate was found to be increased. The complete solution turned black after 4 min and the remaining $NaBH_4$ solution was added completely to speed up the reduction reaction. The mixture was stirred for another 30 min after adding the whole $NaBH_4$ solution. The precipitates were collected using vacuum filtration technique to separate it from the liquid phase. Two sheets of Whatman No 1 filter papers (42 circles, 150 mm diameter) were used in filtration. The filtrated precipitates were washed thrice with absolute ethanol to remove all the water and prevent the rapid oxidation of nZVI. The synthesized nZVI were oven dried at 323 K for 12 hrs. The precipitate was weighed (3.70 g) and stored in a labelled sterile bottle for characterization and adsorption studies.

The equation for the reaction:

$3\ FeSO_4 + 6\ NaBH_4 + 18\ H_2O \rightarrow 3\ Fe^0 + 3\ Na_2SO_4 + 6\ B(OH)_3 + 21\ H_2$

2.6.1 Phytosynthesis of Spondias mombin with Zero-Valent Iron Nano-particle (Sm-nZVI)

Spondias mombin leaves extract (20 mL) was added in drops to 180 mL 0.05 $FeSO_4.7H_2O$ solutions in a 250 mL conical flask on a magnetic stirrer. The clear $FeSO_4.7H_2O$ turned black as soon as the first four (4) drops of plant extract were added. Drops of 1M NaOH solution were added to the reaction mixture to get it up to pH 9. After 1 hr of stirring to ensure proper shape, the reaction mixture was incubated at 333 K in a water bath for 30 min to precipitate the *Sm*-nZVI. The reaction mixture was filtered using two sheets of Whatman No 1 filter papers (42 circles, 150 mm diameter). The resulting *Sm*-nZVI was washed three times with absolute ethanol to eliminate any remaining water and prevent the nanoparticles from oxidizing too quickly. The *Sm*-nZVI synthesized was kept in the oven at 323 K for 12 hrs. The *Sm*-nZVI was collected, weighed (3.08 g) and stored in a labelled sterile bottle for characterization and adsorption studies.

2.7 Characterization of *Sm*-nZVI

Scanning Electron Microscope (SEM), X-ray Diffraction (XRD), and FT-IR Spectrophotometer were used to characterize *Sm*-nZVI.

2.7.1 SEM Analysis

Sm-nZVI was diluted four times in distilled water filtered with two layers of 25 mm Whatman filter paper and ultra-sonicated for 30 min before analysis with SEM. Scanning electron microscope was thereafter used with voltage of 15 KV and at different magnifications.

2.7.2 XRD Analysis

Powdered form of prepared *Sm*-nZVI was analysed using X-ray Powder Diffractometer (XRD). After placing the powdered *Sm*-nZVI in a glass sample holder and scanned, the XRD patterns were recorded at radiation wavelength (Cu-Kα = 1.5405 A°). The angle of diffraction i.e., 2 theta ranged from 5° to 70° at a step size of 0.03°.

2.7.3 FT-IR Analysis

A 50 mg of the stored powdered *Sm*-nZVI was weighed and thoroughly mixed with 250 mg of pure potassium bromide (KBr) with a mortar and pestle for 3 min. Thereafter, 100 mg of the mixed sample was weighed and placed in a KBr die. The die was pressed to produce a pellet using a pair of wrenches. The die with the sample pellets was properly placed in an Infra-Red Spectrophotometer and analysed in the spectral range of 4000-750 cm^{-1}. The spectrum of *Sm*-nZVI was recorded.

2.8 Effect of Different Operating Parameters on Remediation of Contaminated Soil Using Synthesized Nano-sorbent

2.8.1 Effect of Adsorbent Dosage

A solution of contaminated soil was prepared using 5 g of contaminated soil and 50 mL of distilled water and different dosages of *Sm*-nZVI (0.2, 0.4, 0.6, 0.8 g) were added respectively. The mixture was agitated for 30 min and held at 27°C, with a pH 7.0 ± 0.2 and a stirring speed of 200 revolutions per minute (rpm). After that, the mixture was filtered through Whatman No. 1 filter paper. For further study, the filtered solution and residue were placed in separate sterile sample bottles.

2.8.2 Effect of Contact Time

A solution of contaminated soil was prepared using 5 g of contaminated soil and 50 mL of distilled water and 0.2 g of *Sm*-nZVI was added at different contact time namely (15, 45, 60, and 120 min) respectively. The mixture was agitated at 27°C; pH 7.0 ± 0.2 and the stirring of the solution was fixed at 200 rpm. The mixture was then filtered through Whatman No. 1 filter paper The filtered solution and the residue were stored in different sterile sample bottles for further analysis.

2.8.3 Point of Zero Charge

The zero point of charge (pzc) for *Sm*-nZVI was evaluated by dispensing 50 mL of 0.01 M NaCl into 100 mL conical flask and the pH of the mixture adjusted in duplicates to 2.0, 4.0, 6.0, 8.0, 10.0 and 12.0 using 0.1 M NaOH or 0.1 M HCl. A 50 mg of *Sm*-nZVI was dispensed into each of the flask, corked properly and agitated at 180 rpm by mechanical means for 1 hr. It was then allowed to stand for 48 hrs at room temperature. Then, the mixture was filtered and the pH of the supernatant measured and various changes in each pH between initial ($p^H(t_0)$) and ($p^H(t_1)$) obtained. Plot of changes in pH (∆pH) versus initial pH was carried out. The points of intersection were taken as the point of zero charge (Armstrong et al. 2019).

2.8.4 Effect of pH

A solution of contaminated soil was prepared using 5 g of contaminated soil and 50 mL of distilled water and 0.2 g of *Sm*-nZVI was added at different pH namely (3, 7, 9 and 12) respectively. The solution was agitated for 30

min at 27°C with the stirring speed set to 200 rpm. The mixture was then filtered through Whatman No. 1 filter paper The filtered solution and the residue were stored in different sterile sample bottles for further analysis.

2.8.5 Removal Efficiency Calculation

The removal efficiency of the organic pollutants with respect to dosage, contact time and pH was determined using equation 1:

$$\text{Removal Efficiceny } (\%) = \frac{C_o - C_e}{C_o} \times 100 \quad (1)$$

Where, C_o is the initial concentration, and C_e is the equilibrium concentration.

3. Results and Discussion

3.1 Phytochemical screening of aqueous and ethanolic extracts of *Spondia mombin*

The phytochemical screening results of *Spondias mombin* in aqueous and ethanol extracts showed that both extracts contained several bioactive compounds. The presence of alkaloids, flavoniods, tannins, saponins, steroids, and cardiac glycosides were revealed in Table 1. However, tannins and saponins were found in higher concentrations in the aqueous extract than in the ethanolic extract, while alkaloids, steroids, and cardiac glycosides were found in higher concentrations in the ethanolic extract than in the aqueous extract. Phenols were included in the ethanolic extract but not in the aqueous extract. These findings were consistent with those of Ehimwenma and Ehigbai (2015), who detected these bioactive compounds in *Spondias mombin* methanol extracts as well. Moreover, these results also were consistent in part, with the findings of Njoku and Akumefula (2007). The differences between the two findings may be due to the different extraction solvents used and the different regions where the *Spondias mombin* leaves were grown. As a result of the presence of these water-soluble phytochemicals, *Spondias mombin* extract can be used as a reducing and stabilizing agent in the production of zero-valent iron nano-particle (Ghaffari-Moghaddam and Hadi-Dabanlou, 2014).

Table 1: Phytochemical results of aqueous and ethanol extracts of *Spondias mombin*

Solvent	Alkaloids	Flavonoids	Tannins	Saponins	Steroids	Phenols	Cardiac glycosides
Water	+	+	+ + +	+ + +	+	Nil	+
Ethanol	+ + +	+	+	+	+ +	+	+ +

Where, **+ + +** = very highly detected, **+ +** = highly detected, **+** = detected, Nil = not detected

Table 2: Initial average concentrations of PAHs, TPH, and THC in the soil sample

Parameter	Conc. (mg/kg)	Parameter	Conc. (mg/kg)	Parameter	Conc. (mg/kg)
PAHS		**TPH**		**THC**	
Acenaphthene	20.91	C8	9.15		
Acenaphthylene	19.04	C9	8.10		
Anthracene	12.04	C10	15.72		
Benz(a)anthracene	45.31	C11	18.24		
Benzo(b)fluoranthene	73.72	C12	35.86		
Benzo(g,h,i)perylene	50.25	C13	25.19		
Benzo(k)fluoranthene	89.06	C14	39.37		
Chrysene	53.28	C15	43.56		
Fluoreanthene	37.01	C16	35.84		
Fluorene	22.40	C17	52.20		
Naphthalene	17.47	C18	67.52		
Phenanthrene	25.13	C19	67.38		
Pyrene	49.32	C20	115.35		
Benzo(a)pyrene	54.99	C21	136.50		
Dibenz(a,h) anthracene	44.17	C22	134.65		
Indeno(1,2,3-cd)pyrene	40.57	C23	148.07		
		C24	185.37		
		C25	429.66		

		C26	230.96	
		C27	591.60	
		C28	466.78	
		C29	686.96	
		C30	290.81	
		C31	215.02	
		C32	320.80	
		C33	107.57	
		C34	107.97	
		C35	37.23	
		C36	38.82	
		C37	67.80	
		C38	27.56	
		Pr	81.26	
		Ph	61.02	
Total	**654.67**		**4891.65**	**4988.00**

3.2 Initial Concentrations PAHs, TPH and THC in the Crude Soil Sample

Prior to remediation, Gas Chromatography-Flame Ionization Detector (GC-FID) was used to determine the initial concentrations of various contaminants in the crude soil. The results in Table 2 revealed the total concentrations of PAHs, TPH, and THC in the crude soil were 654.67388 mg/kg, 4891.65272 mg/kg and 4988.0 mg/kg. The results further showed that the crude soil was highly contaminated of PAHs and TPH.

3.3 SEM Result of *Sm*-nZVI

The micrograph in Figure 1 revealed a non-uniform particle size and void space. The particles were discovered to be irregular in form, with sizes varying from 13 to 158 nm, with an average particle size of 66.7 nm. The findings were found to be similar to those of Kowshik et al. (2002); Sondia (2004); Kumar et al. (2015), and Sravanthi et al. (2018).

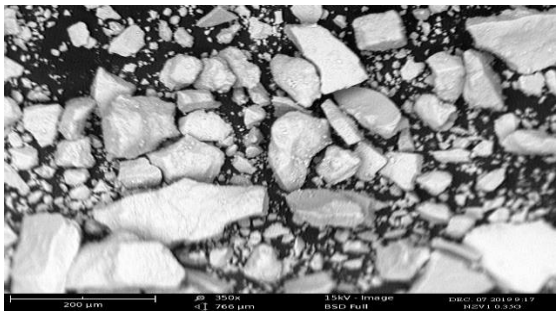

Figure 1: Micrograph of *Sm*-nZVI

3.4 FTIR Interpretation

The spectra results shown in Table 3 present some functional groups such as –OH, -CH, -C=O, N-O, C=C, -COOH, -CN –NH in *Spondias mombin* (*Sm*) and *Spondias mombin*-modified zero-valent iron nanoparticle (*Sm*-nZVI). It was noticed that when moving from *Sm* leaves powder to *Sm*-nZVI, the FTIR spectrum of *Sm* showed vibrational peaks around 3610.86, 3502.86 and 3263.66 cm^{-1} (O-H stretching vibration of phenolic and alcoholic group) which were similar to peaks observed in *Sm*-nZVI around 3610.86, 3518.28, 3271.28 and 3209.66 cm^{-1}, only a slight difference at the ligating sites shows that bioactive molecules adsorption on the iron occurred. The peaks found around 2931.9 and 2885.6 cm^{-1} were ascribed to the -C-H stretching vibration of alkane group in the FT-IR spectrum of *Sm* were similar to that *Sm*-nZVI around 2931.9 and 2870.17cm^{-1} but there was a shift from 2885.6 cm^{-1} to 2870.17cm^{-1} between *Sm* and *Sm*-nZVI with decreasing intensity also showing a stabilization between *Sm* and *Sm*-nZVI. The existence of a carbonyl group in *Spondias mombin* was revealed by a strong peak about 1720.56 cm^{-1}, while a small difference in the band 1712.85 cm^{-1} revealed the presence of a –C=O stretch of carboxylic acid in *Sm*-nZVI. The slight difference between *Sm*-nZVI and *Sm* may be due to bioactive molecules in *Spondias mombin* interacting with ferrous ions through their oxygen donor atoms and being adsorbed on the metal ions surfaces, resulting in a decrease in peak intensities of band observed in *Sm*-nZVI. The C=C stretching vibration of an alkene was observed at peak 1643.41 and 1651.12 cm^{-1} in *Sm* and *Sm*-nZVI. The N-H stretching of the aromatic amino group is responsible for the peaks observed around 1435.09 cm^{-1} in *Sm* and *Sm*-nZVI. Also, the peak at 1242.2 cm^{-1} in *Sm* and *Sm*-nZVI was most likely due to –C-N stretching of an amine of the alkaloids present in *Spondias mombin*. In *Sm* and *Sm*-nZVI, the peaks at 1072.46, 1087.89, and 1103.32 cm^{-1} respectively correspond to –C-O stretching vibration of primary alcohol, –C-O stretching vibration of secondary alcohol and –C-O stretching vibration of secondary alcohol. Interactions between the functional groups in *Sm* and the *Sm*-nZVI were indicated by the change in frequency bands between 1072.46 cm^{-1} and 1087.89 cm^{-1}respectively. The findings in this

study were very close to those of Adeyemi et al. (2020) and Monalisa *et al*. (2013). The existence of phytochemicals such as alkaloids, phenolic, flavoniods, and others in the *Spondias mombin* leaves extract in the *Sm*-nZVI, which were responsible for reducing and stabilizing as well as the capping effect on the nanoparticles, was supported by the occurrence of related frequency bands or peaks in the FT-IR spectra (Sorbiun et al., 2018).

Table 3: Vibrational bands of *Spondias mombin* (*Sm*) and *Spondias mombin*-modified zero-valent iron nanoparticle(*Sm*-nZVI)

Wavenumber (cm^{-1})	Functional groups	Wavenumber (cm^{-1})	Functional groups
	Sm		***Sm*-nZVI**
3610.86, 3502.86, 3263.66	O-H stretching vibration of alcoholic and phrnolic groups	3610.86, 3518.28, 3209.66	O-H stretching vibration of alcoholic and phrnolic groups
2932.9, 2885.6	C-H stretching vibration of alkanes	2931.9, 2870.17	C-H stretching vibration of alkanes
1720.56	C=O carbonyl stretching vibration	1712.85	C=O carbonyl stretching vibration of carboxylic acids
1643.41	C=C stretching vibration of alkenes	1651.12	C=C stretching vibration of alkenes
1519.96	N-O stretching vibration of aromatic nitro-compounds	1519.96	N-O stretching vibration of aromatic nitro-compounds
1435.09	N-H stretching vibration of aromatic amino groups	1435.09	N-H stretching vibration of aromatic amino groups
1242.2	C-N stretching vibration of an amine	1242.2	C-N stretching vibration of an amine
1072.46	C-O stretching vibration of primary alcohols	1087.89	C-O stretching vibration of secondary alcohols
887.28	C=C bending vibration of alkenes	879.57	C=C bending vibration of alkenes

3.5 XRD results of *Sm*-nZVI

The crystal structure and size of the synthesized nanoparticles were ascertained using XRD. The peak at 2θ equal to 44.9° in Figure 2 indicates the presence of zero-valent iron (Fe^{o}) in *Sm*-nZVI. The results of the XRD study of *Sm*-nZVI at 2θ = 34° peak revealed the presence of Fe_2O_3 or Fe_3O_4 in *Sm*-nZVI. Other peaks indicate iron oxyhydroxides and organic matter on the surface of *Sm*-nZVI. The result obtained was found to be very similar to those of Singh et al. (2011); Khasim et al. (2011); and Saranya et al. (2017).

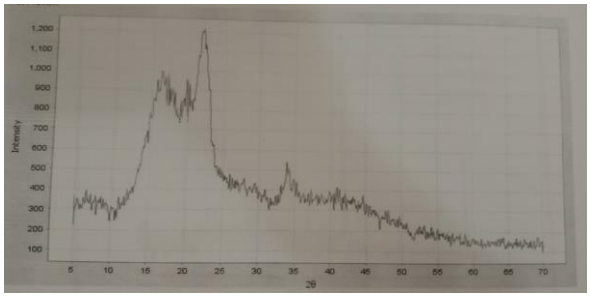

Figure 2: XRD image of *Sm*-nZVI

3.6 Effect of Adsorbent Dose

The result revealed that removal efficiencies (%) changed according to adsorbent dose in Figure 3. The removal efficiencies (%) increased from 40.88 to 44.77, 53.99 and 79.15% as the amount of *Sm*-nZVI was increased from 0.2, 0.4, 0.6 and 0.8 g respectively for THC. The same trend occurred for TPH i.e. the removal efficiencies (%) increased from 40.75 to 75.81, 79.14 and 80.36% as *Sm*-nZVI dosage was increased from 0.2, 0.4, 0.6 and 0.8 g respectively. For PAHs, the removal efficiencies (%) also increased from 95.72 to 96.53, 96.62 and 97.31% as the *Sm*-nZVI dosage was increased in the same progression of dosage. The results showed that 0.8 g of *Sm*-nZVI was the best dosage for achieving the highest removal efficiencies (%) of THC, TPH, and PAHs with 79.15, 80.36, and 96.62%, respectively. Higher doses of *Sm*-nZVI provided more active sites due to the greater surface area, which speed up the reaction. Higher doses of *Sm*-nZVI also resulted in the development of more ferrous ions, which resulted in higher THC, TPH, and PAHs degradation. The above findings were

found to be close to other findings in the remediation of PAH-polluted soil (Pardo et al., 2016).

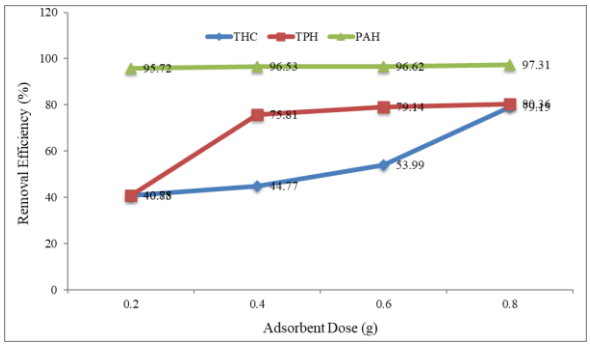

Figure 3: Dosage plots of THC, TPH and PAHs removal (%) using *Sm*-nZVI

3.7 Effect of Contact Time

The result in Figure 4 revealed that for 15, 45, 60 and 120 min, the initial concentration of THC was reduced from 4988.0 mg/kg to 2633, 1366, 878 and 799 mg/kg and, with removal efficiencies of 47.21, 72.61, 82.40 and 83.98% respectively. TPH reduced from 4891.0 mg/kg to 1465.6, 1341.6, 796.8 and 707.2 mg/kg for 15, 45, 60 and 120 min with removal efficiencies of 70.03, 72.57, 83.71 and 85.54 mg/kg respectively. PAHs reduced from 654.7 mg/kg to 25.78, 14.00, 17.76 and 25.51 mg/kg for 15, 45, 60 and 120 min with removal efficiencies of 96.06, 97.86, 97.28 and 96.10%. The removal efficiencies (%) were found to be time-dependent and the effective time for optimum removal efficiencies of 83.93% and 85.54% respectively for THC and TPH was 120 min while the effective time for optimum removal efficiency of 97.86% for PAHs was 45 min. Similar finding was found by Pardo et al. (2016). This study also revealed that PAHs was selectively removed with removal efficiencies ranging from 97.28-97.86%.

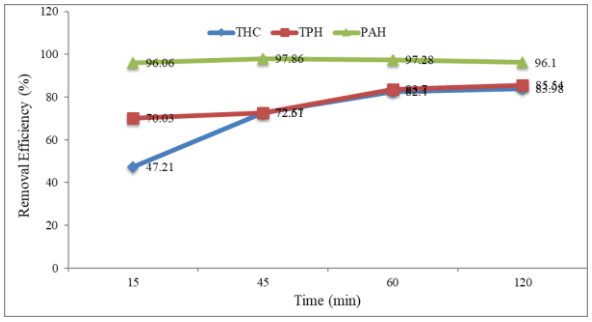

Figure 4: Time plots of THC, TPH and PAHs removal (%) using *Sm*-nZVI

3.8.1 Point of Zero Charge

The point of zero charge for *Sm*-nZVI as represented in Figure 5 was obtained at pH of 3.0. This result demonstrates maximum interaction between *Sm*-nZVI and the organic pollutants at pH of 3.0.

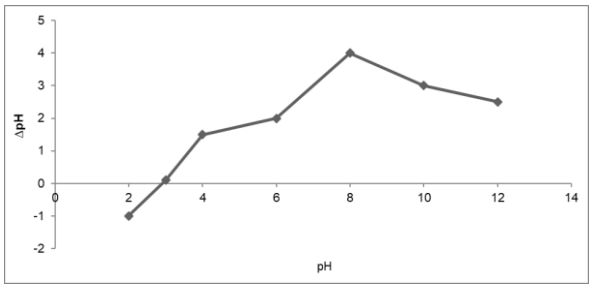

Figure 5: Plot ΔpH versus initial pH for *Sm*-nZVI

3.8.2 Effect of pH

The result in Figure 6 revealed that the total hydrocarbons content (THC) reduced from 4988 mg/kg to 1098, 1498, 1638 and 1560 mg/kg for pH 3, 7, 9 and 12 with removal efficiencies of 77.99%, 69.96%, 67.19% and 68.72% respectively. In the same vein, TPH reduced from 4891 mg/kg to 1192.8, 1584.8, 1753.2 and 1607.6 mg/kg for pH 3.0, 7.0, 9.0 and 12.0 respectively with removal efficiencies of 75.61%, 67.60%, 64.15% and 67.15%. Also, PAHs reduced from 654.7 mg/kg to 19.77, 24.70, 27.16 and 42.24 mg/kg for the same pH as mentioned above with removal efficiencies of 96.98, 96.33, 95.85 and 93.55% respectively. Results showed that maximum removal efficiencies occurred at pH of 3.0 with 96.98%, 77.99% and 75.61% for PAHs, THC and TPH respectively. This behaviour was concordant with the point of zero charge (pzc) value suggesting no strong interaction between hydrogen ion (H^+) and the organic pollutants. Similar result was obtained by Chen (2016). In other words, the removal of organic contaminants was favoured under acidic condition.

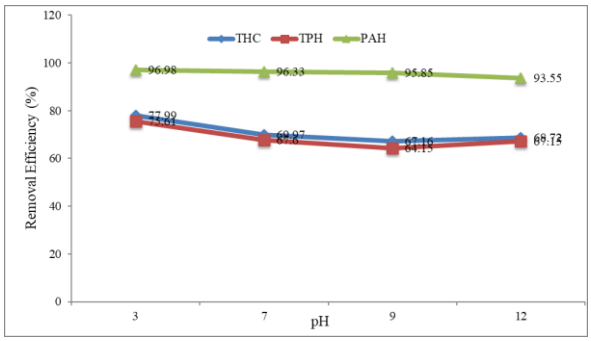

Figure 6: pH plots of THC, TPH and PAHs removal (%) using *Sm*-nZVI

4. Conclusion

The result of the batch studies successfully suggested that biosynthesized zero-valent iron nano-particle has unique decontamination characteristics for THC, TPH, and PAHs

respectively. The performance of the modified nano-sorbent varied significantly according to the experimental parameters used such as adsorbent dosage, contact period or agitation time and pH. The findings obtained from this study revealed that the optimum conditions for the removal of PAHs, THC, and TPH were established at 0.8 g for dosage, 45 min for PAHs and 120 min for THC and TPH while pH of 3.0 for all the three pollutants. The result further revealed that the PAHs was best removed using modified nano-sorbent. This discovery has shown that green nano-sorbent can be effective in the remediation of organic-ladened soils.

Conflict of Interest

The authors declare that there is no conflict of interest.

References

Adejoro, F., and Oguntimehin, I. (2017). Heavy metal pollution of auto-mechanic workshop soils within Okitipupa, Ondo State, Nigeria. *Academia J. Environ. Sci.*, *5*(12), 215-223. https://doi.org/10.15413/ajes.2017.0131.

Ari, H. A., Alani, O. A., Zeng, Qr. *et al.* (2022). Enhanced UV-assisted Fenton performance of nanostructured biomimetic α-Fe_2O_3 on degradation of tetracycline. *J. Nanostruct. Chem., 12,* 45–58. https://doi.org/10.1007/s40097-021-00400-1.

Adeyemi, D. K, Adeluola, A. O., Akinbile, M. J., Johnson, O. O., and Ayoola, G. A. (2020). Green synthesis of Ag, Zn and Cu nano-particles from aqueous extract of *Spondias mombin* leaves and evaluation of their antibacterial activity. *Afri. J. Clinical Expt. Micro., 21*(2), 106-113. https://doi.org/10.4314/ajcem.v21i2.4.

Alani, O. A., Ari, H. A., Alani, S. O., Offiong, N-A. O., and Feng, W. (2021). Visible-Light-Driven Bio-Templated Magnetic Copper Oxide Composite for Heterogeneous Photo-Fenton Degradation of Tetracycline. *Water*, *13*, 1918. https://doi.org/10.3390/w13141918.

Association of Official Analytical Chemists (AOAC) (1990). “Official Methods of Analysis”, 14 Ed., Arlington, V.A., *67*, 503-515.

American Society for Testing Materials ASTM)-D7678 (2017 Edition): Standard Test Method for Total Oil and Grease (TOG) and Total Petroleum Hydrocarbons (TPH) in Water and Wastewater with Solvent Extraction.

Barnes, R. J., Riba, O., and Singer, A. C. (2010). Inhibition of biological TCE and sulphate reduction in the presence of iron nano-particles. *Chemos., 80*, 554-562. https://doi.org/10.1016/j.chemosphere.2010.04.033.

Bhatia, A., Singh, S. D., and Kumar, A. (2015). Heavy metal contamination of soil, irrigation water and vegetables in pri-urban agricultural areas and markets of Delhi. *Water Environ. Res., 87*(11), 2027-2034. https://doi.org/10.2175/106143015X14362865226833.

Cachada, A., Duarte, A., and Rocha-Santos, T. (2018). Soil solution; from monitoring to remediation. *Soil Use Manage.*, *34*(3), 437-438. https://doi.org/10.1111/sum.12443.

Chen, W. (2016). Investigation of Heavy metal (Cu, Pb, Cd and Cr) stabilization in river sediment by nano-zero-valent iron/activated carbon composite. *Environ. Sci. Pollut. Res., 23*, 1460-1470. https://doi.org/10.1007/s11356-015-5387-5.

Curiel, Y. J, Ma, S., and Baldocchi, D. D. (2009). Plant-soil interactions and acclimation to temperature of microbial-mediated soil respiration may affect predictions of soil CO_2 efflux. *Biogeochem., 98*, 127-138. https://doi.org/10.1007/s10533-009-9381-1.

Dermont, G., Bergeron, M., and Mercier, G. (2008). Soil washing for metal removal: A review of physical/chemical technologies and field applications. *J. Hazard. Mater., 152*, 1–31. https://doi.org/10.1016/j.jhazmat.2007.10.043.

Ehimwenma, S. O., and Ehigbai I. O. (2015). Comparative Studies on the Phytochemical Composition, Phenolic Content and Antioxidant Activities of Methanol Leaf Extracts of *Spondias mombin* and *Polyathialongifolia*. *Jord. J. Biol. Sci., 8*(2), 145-149. https://doi.org/10.12816/0027561

FAO and ITPS (2015). Status of the World’s Soil Resources (SWSR) - Main Report. Rome, Italy, food and Agriculture Organization of the United Nations and Inter-Governmental Technical Panel on Soils. http://www.fao.org/3/a-i5199e.pdf.

Ghaffari-Moghaddam, M., and Hadi-Dabanlou, R. (2014). Plant mediated green synthesis and antibacterial activity of silver nano-particles using *Crataegus douglasii* fruit extract. *J. Ind. Eng. Chem.*, *20* (2), 739-744. https://doi.org/10.1016/j.jiec.2013.09.005.

Gill, L. S. (1992). *Ethnomedical uses of plants in Nigeria*. UNIBEN Press, Nigeria, p. 220.

Gil-Diaz, M., Diez-Pascual, S., Gonzalez, A., and Alonso, J. (2016). A nano-remediation strategy for the recovery of an As-polluted soil. *Chemos.*, *149*, 137–145. https://doi.org/10.1016/j.chemosphere.2016.01.106.

Gong, X., Haung, D., Liu, Y., Zeng, G., Wang, R., Wan, J., Zhang, C., Cheng, M., Qin, X., and Xue, W. (2017b). Stabilized nano-scale zero-valent iron mediated cadmium accumulation and oxidative damage of *Boehmeri anivea* (L.) Gaudich cultivated in cadmium contaminated sediments. *Environ. Sci. Technol., 51*(19), 11308-11316. https://doi.org/10.1021/acs.est.7b03164.

Ha, H., Olson, J., Bian, L., and Rogerson, P. A. (2014). Analysis of heavy metal sources in soil using kriging interpolation on principal components. *Environ. Sci. Technol., 48*(9), 4999–5007. https://doi.org/10.1021/es405083f.

Harborne, J. B., and Baxter, H. (1993). Phytochemical Dictionary and Handbook of Bioactive Compounds from Plants. Taylor and Francis, London.

Hu, G., Li, J., and Zeng, G. (2013). Recent development in the treatment of oily sludge from petroleum industry: a review. *J. Hazard. Mater., 261*, 470–490. https://doi.org/10.1016/j.jhazmat.2013.07.069.

International Organization of Standardization. (2013). ISO 11074:2015-Soil Quality Vocabulary. https://www.iso.org/standard/59259.html.

Khasim, S., Raghavedra, S., Revanasiddappa, M., Sajjan, K., Sajjan, K., Mohana, L., and Faisal, M. (2011). Characterization and magnetic properties of polyaniline. *Bull. Mater. Sci., 34*(7), 1557-1561. https://doi.org/10.1007/s12034-011-0358-z.

Koul, B., Taak, P. (2018). Chemical methods of soil remediation. In: biotechnological strategies for effective remediation of polluted soils. Springer, Singapore. https://doi.org/10.1007/978-981-13-2420-8_4

Kowshik, M., Ashtaputre, S., Sharmin, K., Vogel W., and Urban J. (2002). Extracellular synthesis of silver nanoparticles by a silver-tolerant yeast strain MKY3. *Nanotechnol., 14*(1), 95. https://doi.org/10.1088/0957-4484/14/1/321.

Kumar, R., Singh, S., and Pandey, N. (2015). Potential of green synthesized zero-valent Iron nano-particles for the remediation of lead-contaminated water. *Inter. J. Environ. Sci. Technol.*, *12*(12), 3943-3950. https://doi.org/10.1007/s13762-015-0751-z.

Lacatusu, R. (2000). Appraising Levels of Soil Contamination and Pollution with Heavy Metals. In: Heineke, H.J., Eckelmann, W., Thomasson, A.J., Jones, R.J.A., Montanarella, L. and Buckley, B., Eds., European Soil Bureau-Research Report No. 4, 393-403.

Lemaire, J., Bues, M., Kabeche, T., Hanna, K., and Simonnot, M-O. (2013). Oxidant selection to treat an aged PAH contaminated soil by in situ chemical oxidation. *J. Environ. Chem. Eng.*, *1*(4), 1261–1268. https://doi.org/10.1016/j.jece.2013.09.018.

Leon, I., and Shaw, P. E. (1990). *Spondias*: The red *mombin* and related fruits: In Nagy S, Shaw PE and Wardowski WF. Fruits of tropical and sub-tropical Origin-Composition, Properties and Uses. Editorial, pp. 116-126.

Lu, S. F., Wu, Y. L., Chen, Z., Li, T., Shen, C., Xuan, L. K., and Xu, L. (2021). Remediation of contaminated soil and groundwater using chemical reduction and solidification/stabilization method: A case study. *Environ. Sci. Pollut. Res. Int., 28*(10), 12766-12779. https://doi.org/10.1007/s11356-020-11337-3.

Mahmoud, M., Tatiana, M., Svetlana, S., Saglara, M., Gholamreza, N. B., Anatoly, B., and Amit, B. (2021). Effect of nano-materials on remediation of polycyclic aromatic hydrocarbons-contaminated soils: A review. *J. Environ. Manage.*, *284*, 112023. https://doi.org/10.1016/j.jenvman.2021.112023.

Monalisa, P., and Nayak, P. L. (2013). Eco-friendly green synthesis of iron nano-particles from various plant and spices extract*. Inter. J. Plant, Animal Environ. Sci.*, *3*, 68-78. www.ijpaes.com.

Njoku, P. C., and Akumefula, M. I. (2007). Phytochemical and nutrient evaluation of *Spondias mombin* leaves. *Pak. J. Nutri., 6*, 613–615. https://doi.org/10.3923/pjn.2007.613.615.

Nnanake-Abasi, O. O., Opeyemi, K. F., Joseph, P. E., Chaoge, Y., and Jun, D. (2021). Soil washing of total petroleum and polycyclic aromatic hydrocarbons from crude oil-contaminated ultisol using aqueous extracts of waterleaf. *Environ. Technol.,* https://doi.org/10.1080/09593330.2021.1961875.

Pardo, F., Pardo, F., Peluffo, M., Santos, A., and Romero, A. (2016). Fate of iron and polycyclic aromatic hydrocarbon during the remediation of a contaminated soil using iron-activated persulfate; a column study. *Sci. Total Environ.*, *566-567*, 480-488. https://doi.org/10.1016/j.scitotenv.2016.04.197.

Pat-Okunbor, A. E., Obi, C., and Ibezim-Ezeani, M. U. (2019). Equilibrium and Thermodynamic Studies using Eco-Friendly *Cola lepidota* Seed Resins as Novel

Adsorbents in the Removal of *Pb (II) and Cd (II) Ions from Aqueous System. Pak. J. Sci. Ind. Res., Series A: Phys. Sci., 62 A*(3): 146-156. https://doi.org/10.52763/PJSIR.PHYS.SCI.62.3.2019.146.156.

Paz-Ferreiro, J., Gasco, G., Mendez, A., and Reichman, S. M. (2018). Soil pollution and remediation. *Int. J. Environ. Res. Public Health, 15,* 1657; https://doi.org/10.3390/ijerph15081657.

Saranya, S., Vijayarani, K., and Pavithra, S. (2017). Green synthesis of iron nano-particles using aqueous extract of *Musa ornate* flower sheath against pathogenic bacteria. *Indian J. Pharm. Sci.*, *79*(5), 688-694. https://doi.org/10.4172/pharmaceutical-sciences.1000280.

Shankar, P. D., Shobana, S., Karuppusamy, I., Pugazhendhi, A., Ramkumar, V. S., Arvindnarayan, S., and Kumar, G. (2016). A review on the biosynthesis of metallic nanoparticles (gold and silver) using biocomponents of microalgae: Formation mechanism and applications. *Enzyme Microb. Technol., 95*, 28-44. https://doi.org/10.1016/j.enzmictec.2016.10.015.

Singh, K. P., Singh, A. K., Gupta, S., and Sinha, S. (2011). Optimization of Cr (VI) reduction by zero-valent bimetallic nano-particles using the response surface modeling approach. *Desal. 270*(1-3), 275-284. https://doi.org/10.1016/j.desal.2010.11.056.

Sorbiun, M., Mehr, E. S., Ramazani, A., Malekzadeh, A. M. (2018). Biosynthesis of metallic nanoparticles using plant extracts and evaluation of their antibacterial properties. *Nanochem. Res., 3*(1), 1-16. https://doi.org/10.22036/ncr.2018.01.00.

Sofowora, A. (1993). Medicinal plant and Traditional medicine in Africa, 2nd Edition Ibadan: spectrum Books limited, pp.134-156.

Sondia, I., and Sondi, B. S. (2004). Silver nano-particles as antimicrobial agent: A case study on *E. coli* as a model for Gram-negative bacteria. *J. Coll. Interf. Sci., 275*(1), 177-182. https://doi.org/10.1016/j.jcis.2004.02.012.

Sravanthi, K., Ayodhya, D., and Yardgiri, P. (2018). Green synthesis, characterization of biomaterial supported zero-valent iron nano-particles for contaminated water treatment. *J. Anal. Sci. Technol., 9*(3), 11-18. https://doi.org/10.1186/s40543-017-0134-9.

Tang, W. W., Zeng, G. M., Gong, J. L., Liang, J., Xu, P., and Zhang, C. (2014). Impact of humic/fulvic acid on the removal of heavy metals from aqueous solutions using nano-materials: A review. *Sci. Total Environ., 468*, 1014–1027. https://doi.org/10.1016/j.scitotenv.2013.09.044.

Thapa, B., Kumar, K. C., and Ghimire, A. (2012). A review on bioremediation of petroleum hydrocarbon contaminants in soil. *Kathmandu University J. Sci. Eng. Technol., 8*(1), 164–170. https://doi.org/10.3126/kuset.v8i1.6056.

Vamerali, T., Bandiera, M., and Mosca, G. (2010). Field crops for phytoremediation of metal-contaminated land: A review. *Environ. Chem. Lett.,* 8, 1-17. https://doi.org/10.1007/s10311-009-0268-0.

Wang, S., Chen, S., Wang, Y., Low, A., Lu, Q., and Qui, R. (2016). Integration of organohalide-respiring bacteria and nano-scale zero-valent iron (Bio-nZVI-RD): a perfect marriage for the remediation of organohalide pollutants. *Biotechnol. Adv., 34*, 1384-1395. https://doi.org/10.1016/j.biotechadv.2016.10.004.

Wu, Z., Yuan, X., Zhang, J., Wang, H., and Jiang, L. (2017). Photocatalytic decontamination of wastewater containing organic dyes by metal-organic frameworks and their derivatives. *ChemCatChem, 9*(1), 41-64. https://doi.org/10.1002/cctc.201600808.

Yuting, Q., Caidie, Q., Mengmeng, C., and Sijie, L. (2020). Nanotechnology in soil remediation-applications vs. *implications. Ecotoxicol.* Environ. Safety, *201*, 110815. https://doi.org/10.1016/j.ecoenv.2020.110815.

Zeng, G., Chen, M., and Zeng, Z. (2013). Shale gas: Surface water also at risk. *Nature*, *499*, 154. https://doi.org/10.1038/499154c.

